Analysing the Polarity Reversal near the Cretaceous-Tertiary Boundary by a Well-tried Model

Von G. P. SENDLHOFER, H. J. MAURITSCH, W ZEISSL
Mining-University Leoben, Austria

(Vorgelegt in der Sitzung der math.-nat. Klasse am 15. Oktober 1992 durch das w. M. FRANZ KURT WEBER)

The main goal of this investigation was to apply a model of the reversing geodynamo, near the Cretaceous-Tertiary boundary.

The model is based on the assumptions of non axialsymmetric dipole sources within the core. The Cretaceous-Tertiary boundary (KTB) was sampled and magnetostratigraphically analysed by R. ROCCHIA et al. (1990), LOWRIE and ALVAREZ 1977 (Gubbio-section, Italy) as well as by ZEISSL and MAURITSCH 1989 in Gams (Austria). The available VGP-paths show only little differences in longitude when passing the equator and the transition can be called nearsided. Assuming that the behaviour of the geomagnetic field during a polarity transition is dominated by non-dipol terms (axialsymmetric and not axialsymmetric ones), we applied a flooding model to the observed data (similar to that of K. A. HOFFMAN). For octupole dominated transition-fields we start the onset of the reversal at high latitudes in the core, for quadrupole transition-fields in the northern hemisphere and the Gauss coefficients will be calculated for each field configuration.

The Geological frame

Since the magnetostratigraphic results of Gubbio (Italy) are already published (LOWRIE and ALVAREZ 1977, ROCCHIA et al. 1990) in the present paper just information from the locality Gams are given.

The Gosauian basin of Gams belongs to the eastern part of the Northern Calcareous Alps in Austria. From a local tectonic point of view it is part of the upper austroalpine Ötscher-Decke and can be divided in a western and an eastern part. The eastern part, were the magneto-stratigraphic profil in discussion belongs to, is surrounded by an early Triassic "high" in the west, jurassic Plassenkalk in the north. In the South and East the boundary of the basin is formed by an overthrusting zone (H. KOLLMANN 1964 a, b) (Fig. 1).

The gosauian sediments start in the eastern part of the basin of Gams with upper Santonian overlayn by the so called "deeper marl complex" of lower to early Upper Campanian age. This complex is followed by the Nierntaler beds of late Upper Campanian to Lower Paleocene age, the breccia-sandstone complex of Middle Paleocene and the clay-marl complex of Upper Paleocene.

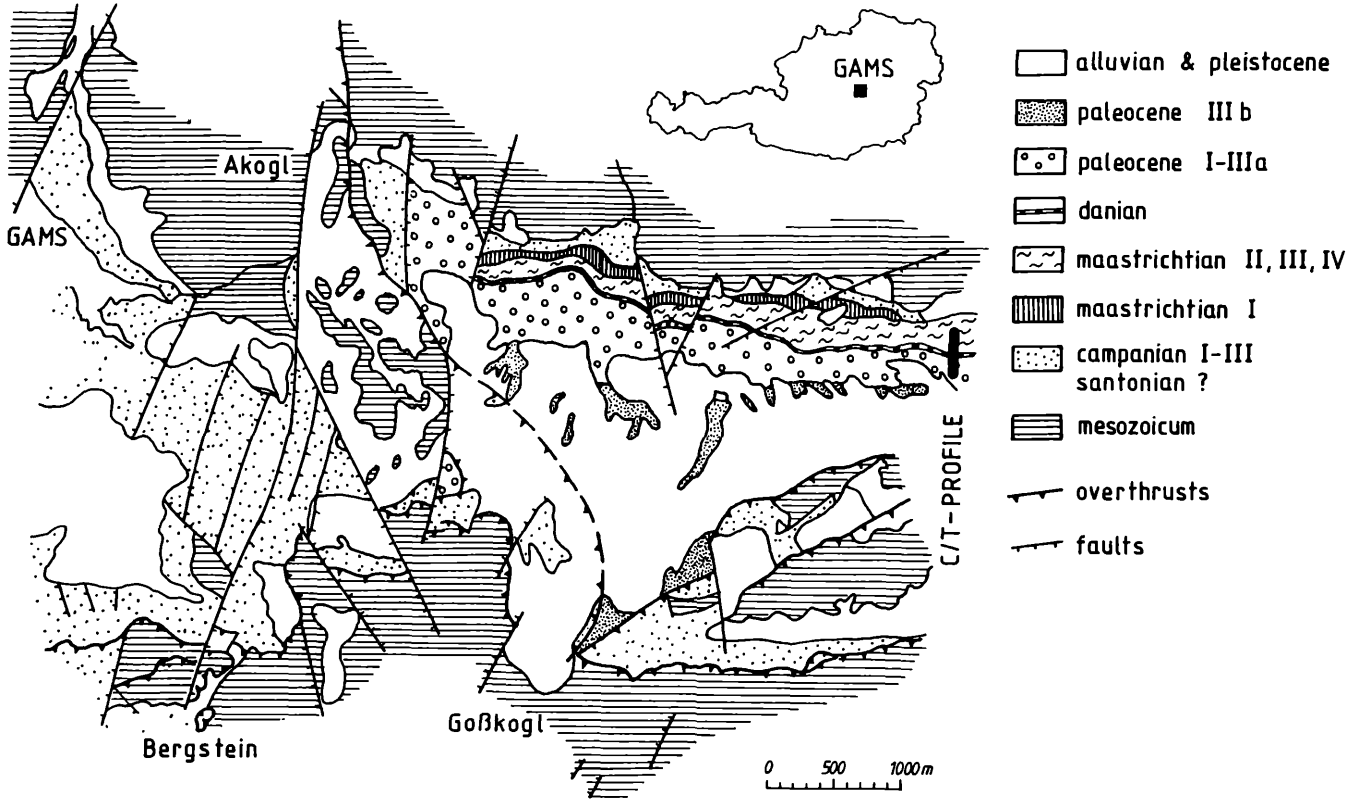

Fig. 1: Simplified geological map of the basin of Gams.

Caused by the Lower Campanian overstrusting of the southern rim, Gosauian sediments were cut of in the Upper Campanian conglomerate and marl horizon and slightly transported to the north.

The studied profile belongs to the Nierntaler beds, which consist of limestones and marls particularely in the Maastrichtian, marls, sand- and siltstones in the Danian. The whole flyschoid sequence is cut by several minor faults with displacements of 5–50 cm but always absolutely reconstructable. Sedimentological investigations (PREISINGER 1990)

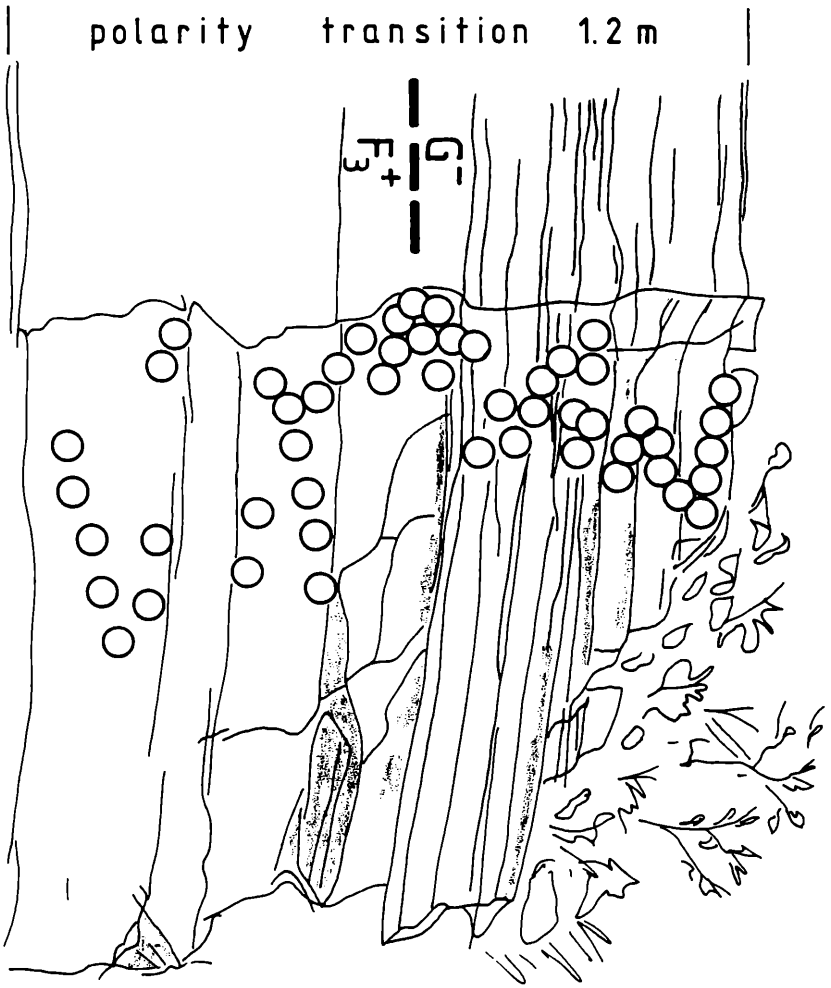

Fig. 2: Scatch of the transition sequence and sample position.

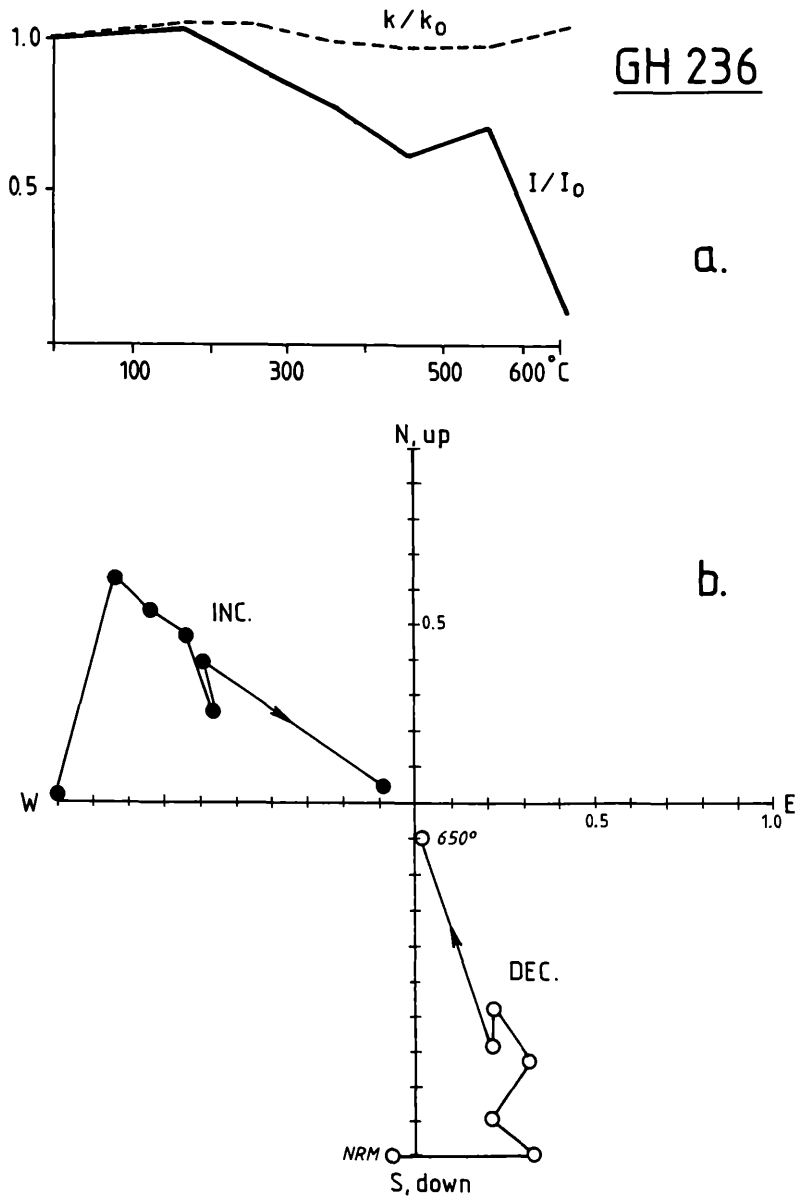

Fig. 3: Rockmagnetic behaviour of the samples above and below the C/T-boundary.
a) Thermal demagnetization of sample GH 236.
b) Modified Zijderveld-plot of GH 236, the intensity is normalized.
c) AC-cleaning of sample GH 332.
d) Modified Zijderveld-plot of GH 332, the intensity is normalized.
e) Saturation acquisition in natural state and after heating up to 200 °C.

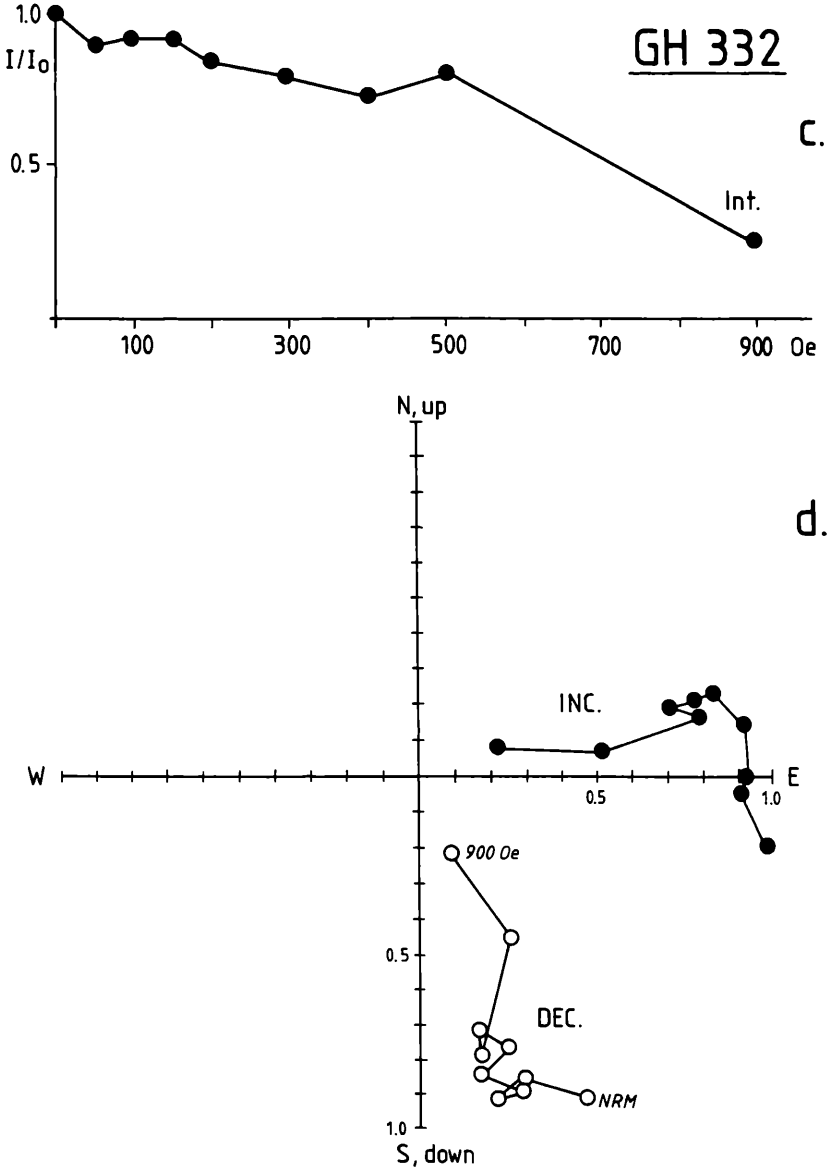
GH 332
c.
1.0
I/I0
0.5
Int.
100
300
500
700
900 Oe
d.
N, up
INC.
W
E
0.5
1.0
900 Oe
0.5
DEC.
NRM
1.0
S, down

Fig. 3c, d

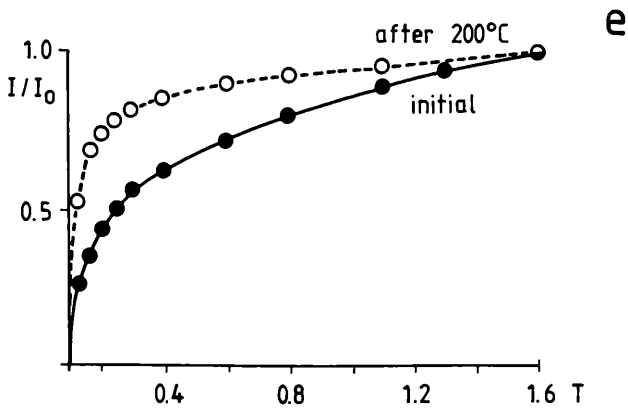

Fig. 3e

described the sediment as being partly of turbiditic and partly hemipelagic origin.

Sampling and rockmagnetic investigations

The sampling was carried out by a portable drill in the Maastrichtian and in the sand/siltstone layers of the Danian. The weak to unconsolidated parts of the Danian were sampled by a special tool, which allows to push a oriented plastic tube into the soil. The tube is marked in the usual paleomagnetic manner with an arrow and a fiducial line and is closed by a lid to prevent drying out of the sample. The extent of the disturbing effects of this sampling technique depends on the grain size of the sample material. The sampling interval varied between 5 and 15 cm for the whole K/T-boundary section, whereas for the detailed polarity section 1.0–1.5 cm (Fig. 2) were chosen. The polarity boundary from G^- to F_3^+ was chosen since the facies, the possibility of drilling and the lack of faults were good pre-conditions.

On a large number of pilots, the rockmagnetic behaviour was studied. As it can be seen in Fig. 3 magnetite as well as haematite and maghaemite can be identified. Up to 150 °C to 200 °C there is also some influence be ironhydroxide which particularly influences the IRM-acquisition in the natural stage. After heating the pilots to 200 °C and repeating the IRM-acquisition there is always a remarkable shift towards soft, magnetite like behaviour (Fig. 3 e).

Anblocking temperatures at about 650 °C and saturation at about 0.5 T is a strong argument for maghaemite whereas hematite is characterized by unblocking temperatures of about 650 °C and saturation above 1.5 T. The susceptibility does not vary much throughout the whole temperature range (Fig. 3 a, b). AC-cleaning was just successful for the "soft" components of the magnetization (fig. 3 c, d); the whole collection was cleaned at three temperature steps.

The NRM-intensities vary from 5 $10^{-5} - 10^{-3}$ A/m.

In the case of very low NRM-intensities, a successful isolation of the true ChRM was not always possible since their intensity was within the noise level of the cryogenic magnetometer.

Magnetostratigraphic results

The whole collection of samples were cleaned in three thermal demagnetization steps, at 200, 300 and 400 °C. Higher cleaning temperatures were chosen, where hematite was clearly identified as main carrier of the ChRM. Using all these results a "best fit" column was produced (Fig. 4). It clearly shows two polarities; normal at the top and the bottom of the section and reversed in the middle part. Since the K/T-boundary was defined by geochemical, mineralogical and biostratigraphical methods (PREISINGER et al. 1990) the reversed zone is identified as G^- zone (chrone 29 R), top one as H (chrone 29 N) and the bottom one as F_3^+ zone (chrone 30 N). In some levels a higher scatter can be seen, which is most probably due to the turbiditic origin of the sediments. Just between 2 and 3.5 m in the Maastrichtian the declination and inclination is changing synchronously that a poleexcursion seems to be very probable. Any other "finger prints" for the G^- zone are missing.

For the modelling of polarity transition, the interval from 11.8 to 13.0 m in the Maastrichtian was chosen. As mentioned above, this part of the profile consists mainly of limestones and marls. The rocks are very suitable for drilling. The cores were drilled with a 30 % overlap of each core (Fig. 2).

Calculating with a sedimentation rate of 1.7 cm/1000 yr. no time interval larger then 200–300 yr could have been missed.

The data underlying the analysis

Besides the data-set from Gams we used for our modelling two data-sets from Gubbio (Italy), which were sampled and magnetostratigraphically analysed by ROCCHIA et al., (1990) Fig. 5, as well as LOWRIE and ALVAREZ (1977) Fig. 6. The inclination and declination values of these studies are shown in Fig. 5–6. We can see that the F_3^+-G^- polarity reversal is normal to reverse transition.

We worked on both the first and second set of data from Gubbio leaving them unchanged, using them without smoothing out anything in advance. However, the data by ROCCHIA et al. show surprisingly small scatter, indicating that the data has already been filtered.

The data of Gams Fig. 7, show a higher scatter obviously due to sedimentary processes as mentioned above.

Non of the possible methods of filtering with respect to the model applied leads to useful results. Therefore we left the data of Gams without any filtering.

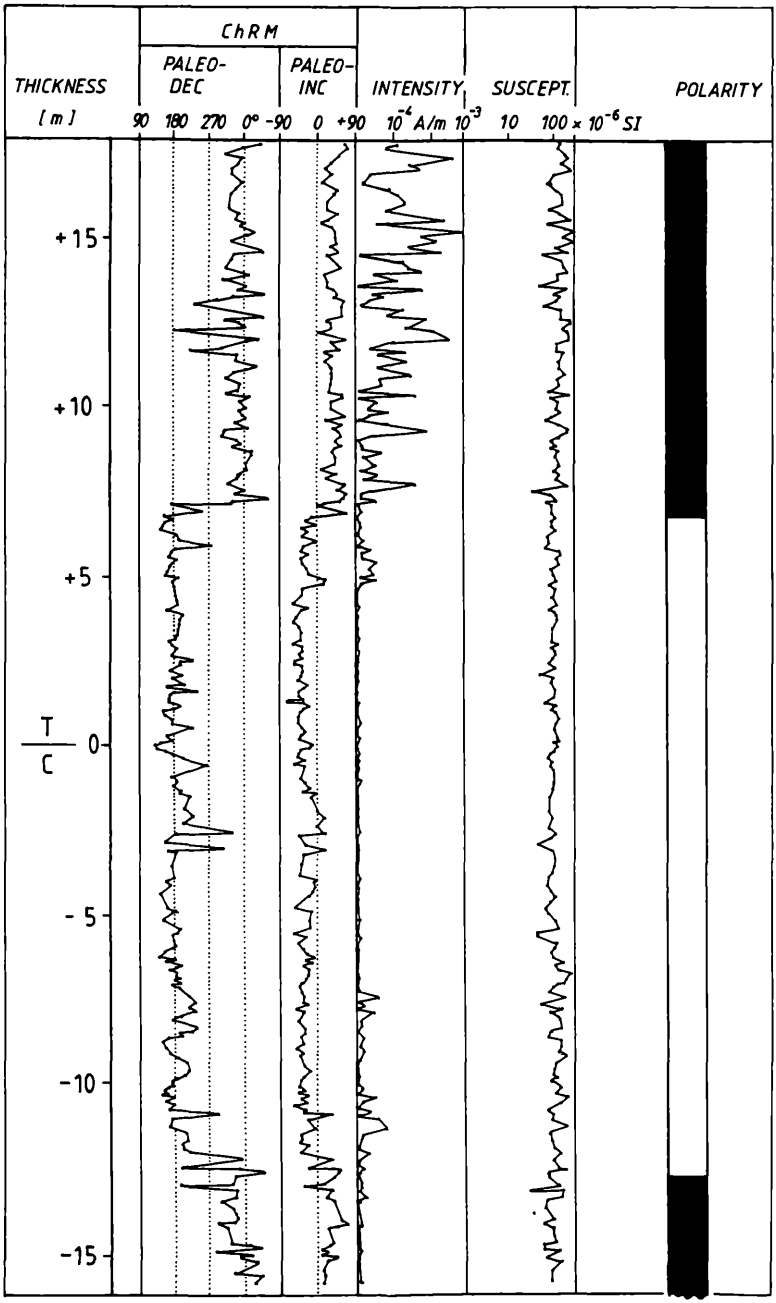

Fig. 4: C/T-boundary profile showing the characteristic remanent magnetization with declination, inclination and intensity, susceptibility and polarity.

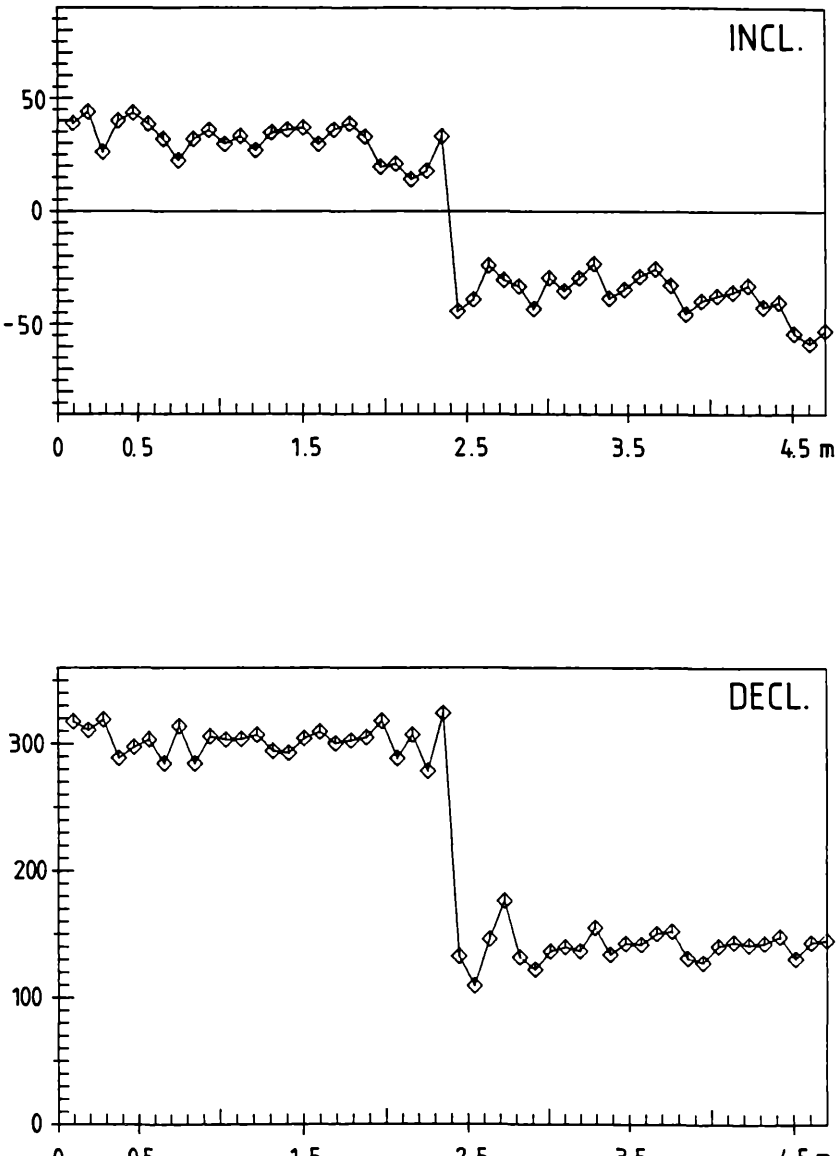

Fig. 5: Inclination and declination values observed from ROCCHIA et al. (Gubbio, Italy).

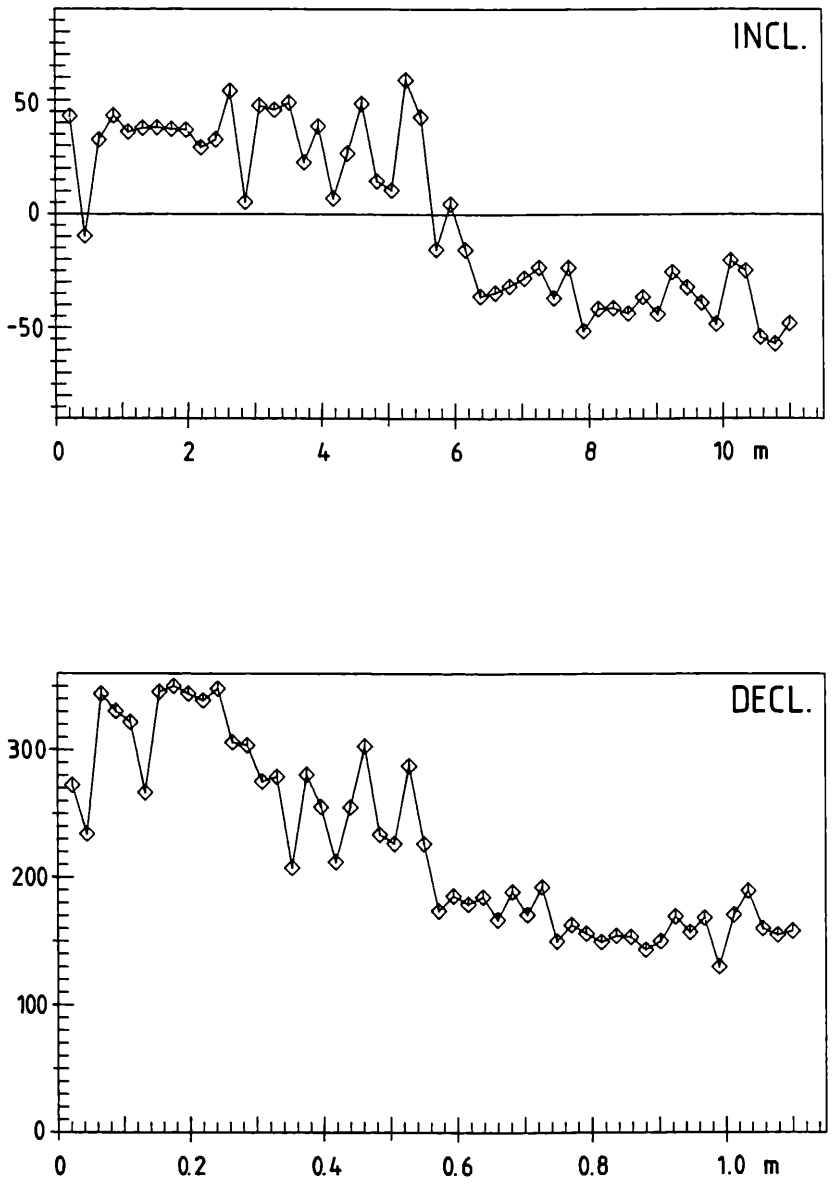

Fig. 6: Inclination and declination values observed from LOWRIE and ALVAREZ (Gubbio, Italy).

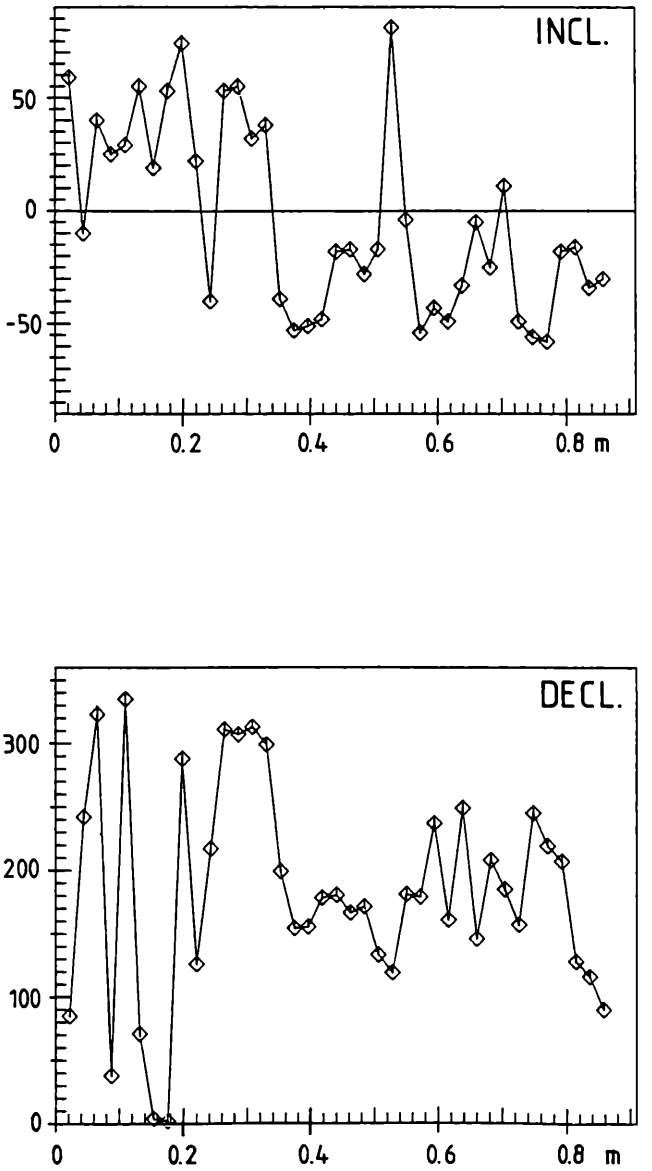

Fig. 7: Inclination and declination values observed from ZEISSL and MAURITSCH (Gams, Austria).

The model

Finally to be able to present the data properly, and to develop a feeling for the Gaussian coefficients of the transition, we used a flooding model, similar to that of KEN HOFFMAN (1979) and (1981), which is discussed briefly.

Within the core, on a certain point of the lateral surface of a cylinder covered with dipoles perturbation is generated. This perturbation spreads in both directions at linear velocity, both vertically and azimuthally, resulting in a reversal of polarity. Depending on the location of the source of the perturbation quadrupolar- and octupolar – dominated transition fields can be generated. The variable parameters of the model are the dimensions of the cylinder, the location of the source of the perturbation, the number of the poles and the vertical step width. The relation between the number of poles and the vertical step width can be compared with the relation of veolocities (v) which results in a specific value (v–1).

Results

Our analysis includes the original, unfiltered data (in general) from the range where the inclination finally changes its sign. As a point of reference for the model we used the transition of the observed VGP-path through the equator.

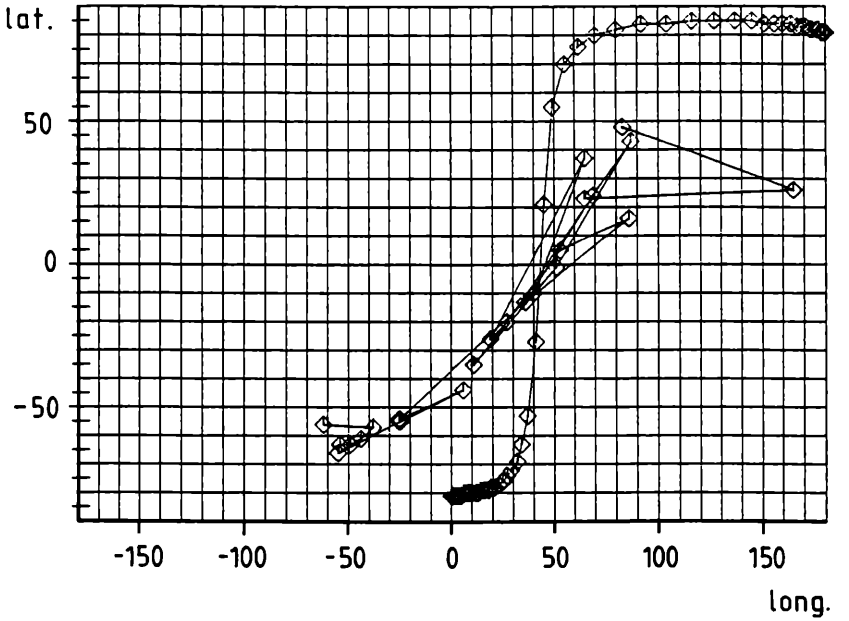

Fig. 8: Model simulation (octupole; perturbation 350° E) for the observed VGP-path from the data-set of LOWRIE and ALVAREZ (site: Gubbio; 43.2° E, 12.3° N).

It is clearly recognizable that the VGP-path and the site are lying within 90° angular distance and can therefore be called nearsided. The fact of a nearsided N–R reversal causes a quadrupole transition field, which starts in the northern hemisphere or an octupole transition field, which starts at high latitudes (FULLER et al. 1979).

Because of the lack of data from the southern hemisphere, we were not able to distinguish between quadrupole and octupole dominated fields. Therefore the model VGP-path are nearly the same for octupole and quadrupole simulated transitions, but depend in our modelling from a different source of perturbation.

For our model we chose a radius r = 0.13 r_e (Earth Radii), and the length of the cylinder L = 0,8 r_e. We took the same dimensions of the cylinder as K. HOFFMAN at discribing the Brunhes-Matuyama polarity reversal.

By appropriately choosing the location of the perturbations, we got the results shown in Fig. 8–10. – All diagrams show only that part of the VGP path in which the transition took place. We achieved satisfactory results as far as the octupole-dominated transition is concerned, at a perturbation source at 350° east.

For the quadrupole-dominated transition we chose an perturbation source at 310°

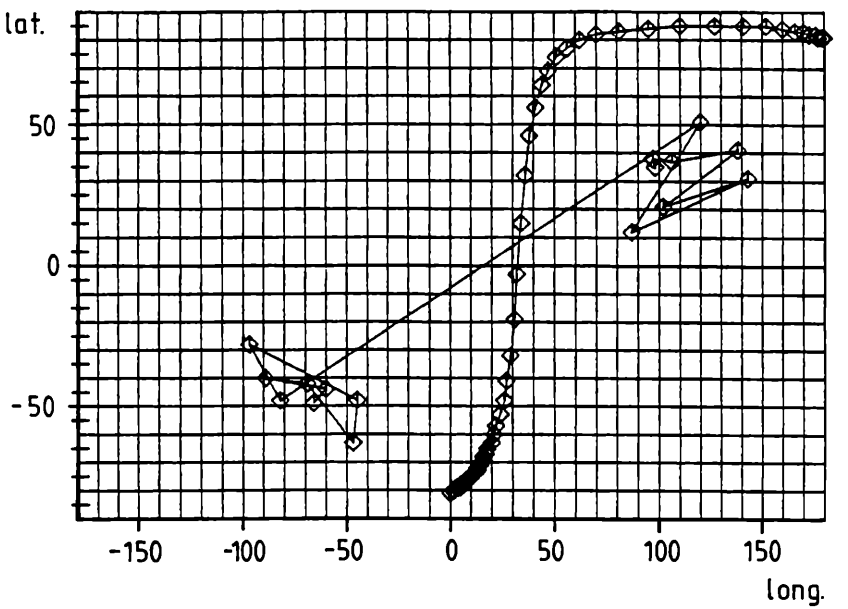

Fig. 9: Model simulation (quadrupole; perturbation 310° E) for the observed VGP-path from the data-set of ROCCHIA et al. (site: Gubbio, 43.2° E, 12.3° N).

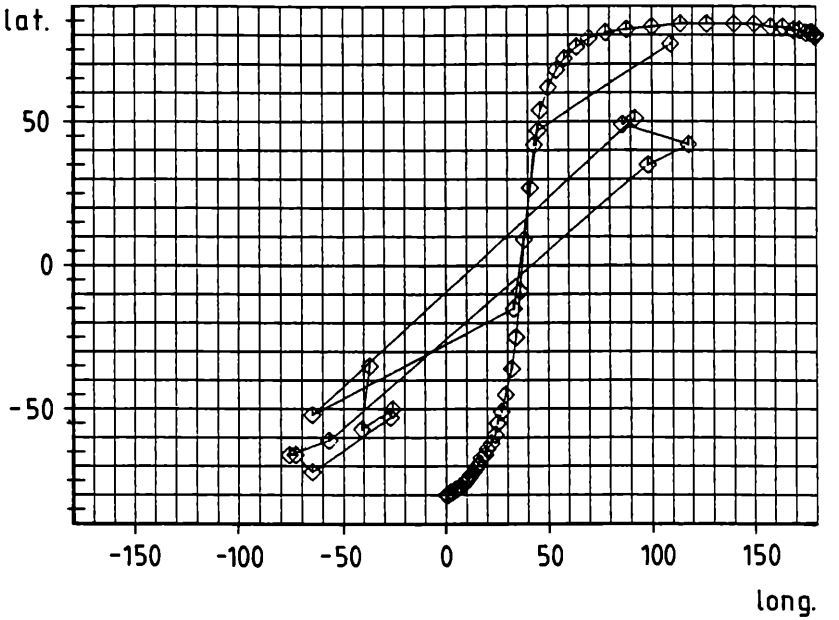

Fig. 10: Model simulation (quadrupole: perturbation 310° E) for the observed VGP-path from the data-set of ZEISSL and MAURITSCH (site: Gams, 46.8° E, 14.6° N).

To achieve a more flat VGP-path we chose the change of the dimensions of the cylinder.

In this case a problem arises, the model VGP-path always starts at 180° east and ends at 0° so that it is nearly impossible to get a good fit with the observed values. In addition a thicker cylinder increases the nonzonal coefficients.

Drawing conclusions as far as the original data is concerned would be rather dubious, because the intersection angle of the observed VGP-path to the meridians are not supposed to be exclusively the consequence of nonzonal non dipole components.

The Gaussian coefficients of the different transitions are shown in Fig. 11–12. For the octupole dominated case, as one can see, the dipole (g_1^0) decreases through zero and the controlling terms are, the octupole (g_3^0), the non axisymmetric quadrupole $([g_2^1]^2+[h_2^1]^2)^{1/2}$ and the higher order term $([g_4^1]^2+[h_4^1]^2)^{1/2}$ (see K. HOFFMAN 1981).

In case of the quadrupole dominated transition, both zonal dipole and octupole terms go to zero while the zonal quadrupole (g_2^0), the non zonal quadrupole $([g_2^1]^2+[h_2^1]^2)^{1/2}$, and higher order terms $([g_4^1]^2+[h_4^1]^2)^{1/2}$, are still existent (Fig. 12).

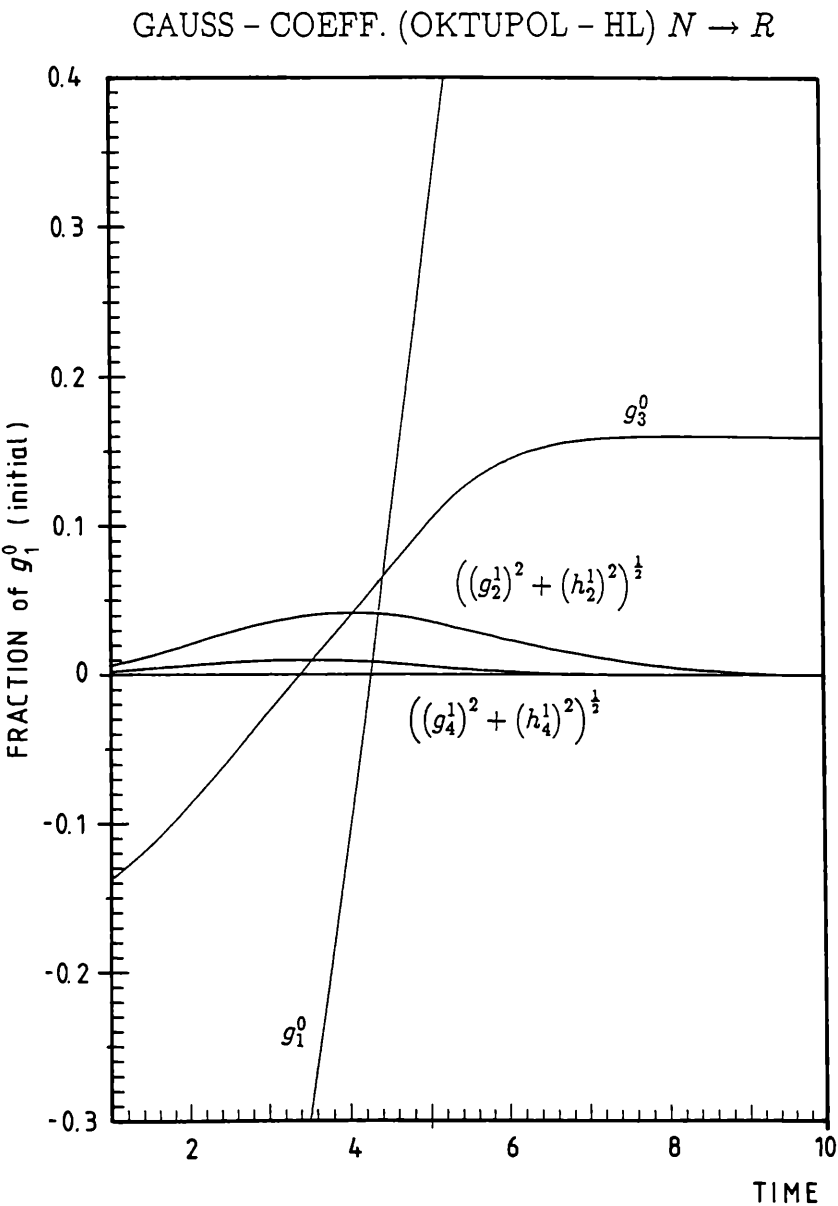

Fig. 11: Schematic description of the harmonic content during a octupole-dominated transition, generated from the model.

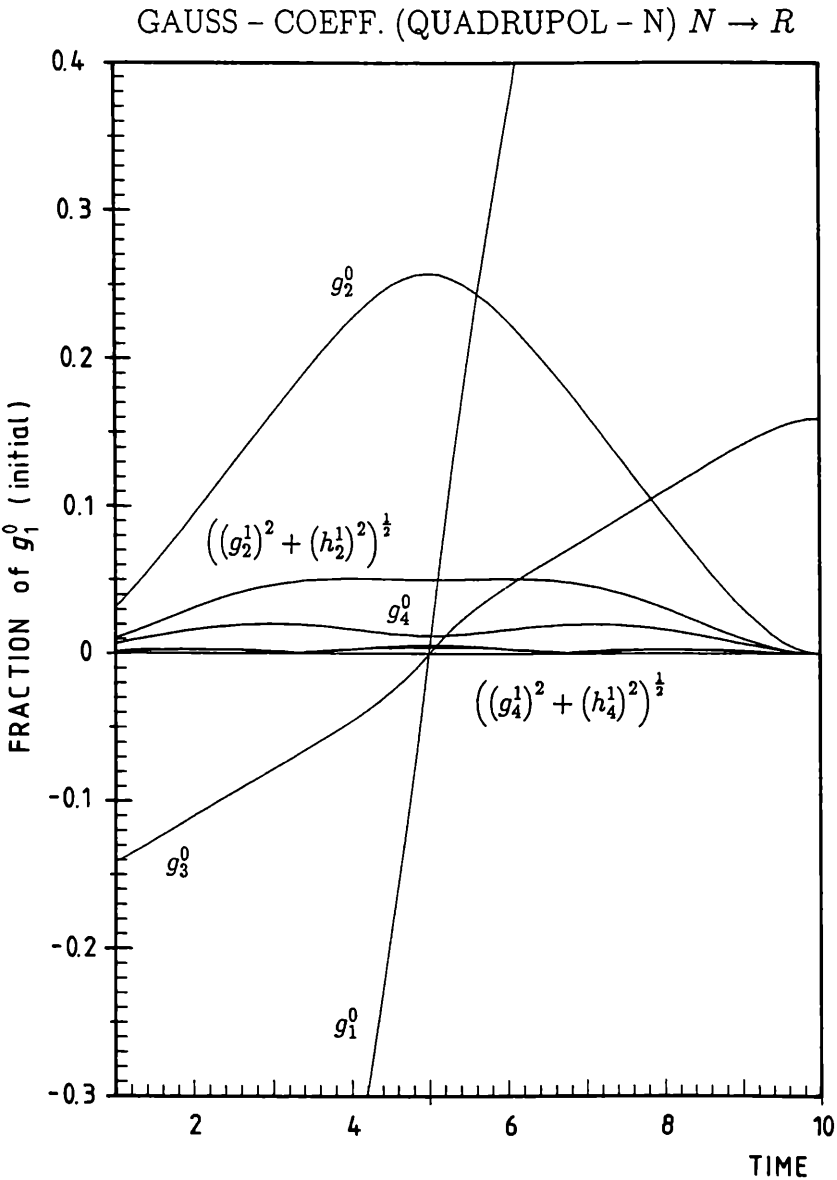

Fig. 12: Schematic description of the harmonic content during a quadrupole-dominated transition, generated from the model.

Discussion

Since numerous current investigations on the K/T boundarys will lead to large number of reliable data sets of the transition G^- to F_3^+, in the present paper the first attempt was made based on three available data sets. As mentioned above these datasets are coming from Gubbio and Gams and have the disadvantage, as far as the modelling is concerned that they are close to each other geographically. The currently investigated sections will help to overcome this problem since one needs at least 3 data points over an angular distance of 180° in longitude for a good estimation.

Another problem during the modelling is the choice of the cylinder dimensions. With regard to the assumption that the cylinder lies within the core one gets different possibilities in choosing the dimensions of this cylinder. But in this case the goal to determine the distribution of the Gauss coefficients with respect to the inclination of the VGP-path to the equator was not reached.

Although all transitions of the observed VGP-path show more or less the same sense of inclination to the equator – the three data-sets are not enough for such an interpretation.

The loop in the data-sets of Gams could be due to an excursion before the actual reversing process starts, even though there is no evidence in the other datasets. The reason for this controversy could be caused by the sample distance, in the case of Gams the sampling density was unusually high so that much more detail can be expected. Anyway the model diagram at the beginning of the reversal shows a close similarity to the data previous to the uncontrolled behaviour. This fit is the result of no filtering. Any common filtering suppresses the higher inclination values and one gets a VGP-path like in Fig. 9.

Future investigations with the same fidelity as Gams should prove whether the loop is a significant fingerprint for this reversal.

Suggestions that many of the VGP-paths from 100.000 yr to 10 Myr are clustered within two meridians have reopened the debate whether the transition field is dipolar or non dipolar (BOGUE, 1991; LAJ et al., 1991). However the VGP-path observed from the K/T boundary does not lie within these meridional bands. Recently, studies have been made in describing the transitional field geometry by using primary (antisymmetric about the equator) and secondary (symmetric about the equator) field families (MCFADDEN et al., 1988; HOFFMAN, 1991). In this case there is no simple distinction between dipole and non-dipole geometries; each family contain both. Maybe this studies will lead to a better description of the harmonic content and find out the dominant Gaussian coefficient during reversal. The harmonic content of the secondary field family could be similar to the distribution of the quadrupole simulated transition.

Acknowledgements

Finally, we'd like to express our thanks towards V. COURTILLOT and to W. LOWRIE for providing their data.

References

BOGUE, S. (1991): Reversals of opinion. Nature, Vol. 351, p. 445.

FULLER, M., WILLIAMS, I., and HOFFMAN, K. A. (1979): Paleomagnetic records of geomagnetic field reversals and the morphology of the transitional fields. Rev. Geophys. Space Phys., Vol. 17, p. 179.

HOFFMAN, K. A. (1979): Behaviour of the geodynamo during reversal: A phenomenological model. Earth Planet. Sci. Lett., Vol. 44, p. 7.

HOFFMAN, K. A. (1981 a): Quantitative description of the geomagnetic field during the Matuyama-Bruhnes polarity transition. Phys. Earth Planet. Int., Vol. 24, p. 229.

HOFFMAN, K. A. (1991): Long-lived transitional states of the geomagnetic field and the two dynamo families. Nature, Vol. 354, p. 273.

LAJ, C., MAZAUD, A., WEEKS, R., FULLER, M., HERRERO-BERVERA, E. (1991): Geomagnetic reversal paths. Nature, Vol. 351, p. 447.

LOWRIE, M., and ALVAREZ, E. (1977): Upper-Cretaceous-Paleocene magnetic stratigraphy at Gubbio, Italy, III. Upper Cretaceous magnetic stratigraphy. Geol. Soc. Am. Bull., Vol. 88, p. 374.

ROCCHIA, R., BOCLET, D., BONTE, PH., JEHANNO, C., YANCHEN, COURTILLOT, V., MARY, C., and WEZEL, F. (1990): The Cretaceous-Tertiary boundary at Gubbio revisited: vertical extent of the Ir anomaly. Earth Planet. Sci. Lett., Vol. 99, p. 206–219.

ZEISSL, W., and MAURITSCH, H. J. (1988): Magnetostratigraphy of a new K/T boundary in the Gosau beds of Austria. Ber. d. Geol. B.-A., Bd. 15.

ZEISSL, W (1989): Magnetostratigraphie an geologischen Zeitgrenzen in den Karnischen Alpen und Nördlichen Kalkalpen. Unpubl. PhD Thesis, Montanuniversität Leoben.